

# RAPID EARTHQUAKE LOSS ASSESSMENT: STOCHASTIC MODELLING AND AN EXAMPLE OF CYCLIC FATIGUE DAMAGE FROM CHRISTCHURCH, NZ

John B. Mander<sup>1</sup>, Geoffrey W. Rodgers<sup>2</sup>, and David Whittaker<sup>3</sup>  
Texas A&M University<sup>1</sup>, University of Canterbury<sup>2</sup>, and Beca Consultants<sup>3</sup>  
College Station, Texas, USA<sup>1</sup> and Christchurch, New Zealand<sup>2,3</sup>

## Abstract

Low-cycle fatigue demands on the reinforcing steel in concrete structures has been brought to the forefront due to the numerous earthquakes of the 2010-2011 Canterbury Earthquake and Aftershock Sequence. Post-event structural assessment requires methods to rapidly assess the proportion of a structure's fatigue life that has been consumed by an earthquake and aftershock sequence to determine restoration/remediation requirements. First, the structural fatigue capacity is assessed for a nonlinear ductile structural response. Second, time-history analysis and cycle counting methods are used to determine the cumulative low cycle fatigue demand imposed upon a structure by the Earthquake Sequence for the Christchurch CBD. Results are presented as fatigue demand spectra. The effect of the fatigue demand is then assessed for a bridge structure conforming to New Zealand design code provisions. Case study results show the Canterbury Earthquake Sequence consumed varying degrees of fatigue life, up to and including fracture. As low cycle fatigue damage is not repairable, the damaged portions and their associated connections within the structure require replacement and reconstruction in order to fully restore the structure to a new condition.

## Introduction

Large earthquakes induce a number of cycles of vibration of varying amplitude. Particularly under inelastic seismic response, such vibrations cause progressive damage and deterioration of resistance. Moreover, even a moderate level earthquake may also strain the reinforcing steel beyond its elastic limit thereby causing yield and permanent damage. As mild steel reinforcing bars generally possess a large reserve (monotonic) strain capacity, one-time yielding is generally not considered a serious issue. However, if the structure has sustained several post-yield cycles of loading, even though the concrete may be repairable, there remains substantial seismic induced fatigue damage to the reinforcing steel. Although restoration is required, seismic-induced fatigue damage to reinforcing steel is generally irreparable; the phenomenon is known as 'low cycle fatigue', representing a low number of large strain amplitude cycles.

While modern seismic loading codes carefully consider the onset of plastic deformation within a structure and provide levels of acceptable damage through limit states design, the long-term implications of such expected damage, in terms of cyclic fatigue failure, are not well considered. Structural fatigue considerations have been highlighted most recently in the Canterbury region of New Zealand, where an atypically long earthquake and aftershock sequence has placed significant cyclic demands on the region's structures. The post-earthquake restoration of damaged structures requires an assessment of the degree of damage sustained and measures whereby the structure may be restored to a substantially as new condition.

This paper presents an investigation into the cumulative cyclic fatigue demand on a structure from the 2010-2011 Canterbury (New Zealand) earthquake and aftershock sequence for the Christchurch CBD where a composite of the four strong motion recording stations within the CBD are used in an aggregate sense, are used. Estimates of the cumulative fatigue demand across the all major events from the 2010-

2011 Canterbury Earthquake Sequence are assessed and compared with the cyclic fatigue capacity of a bridge structure that has been designed to New Zealand standards.

### Structural Fatigue Capacity

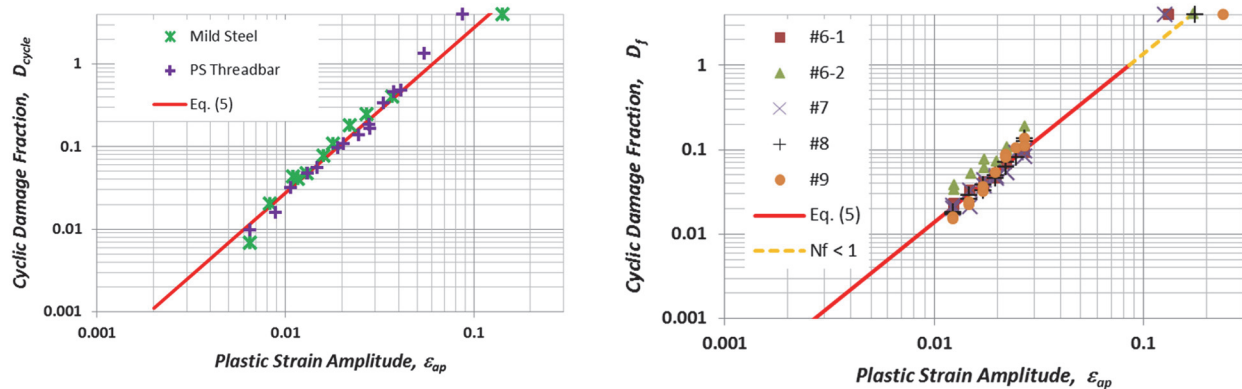
Low cycle fatigue results from Mander et al. (1994) show for both mild steel reinforcing bars and for high-strength high-alloy prestressing threadbars ( $f_y = 870$  MPa yield strength), a general fatigue-life relationship may be given by:

$$\varepsilon_{ap} = 0.08(2N_f)^{-0.5} \quad (1)$$

The inverse of the number of cycles to failure ( $N_f$ ), may be defined as the fatigue damage for one cycle of loading at the plastic strain amplitude ( $\varepsilon_{ap}$ ), thus  $D_{cycle} = 1/N_f$ . Therefore, inverting Equation (1) and generalizing the result one obtains

$$D_{cycle} = \frac{1}{N_f} = \left| \frac{\varepsilon_{ap}}{\varepsilon_{pf}} \right|^2 \quad (2)$$

in which  $\varepsilon_{pf}$  is defined as the plastic fatigue strain (the plastic strain that would lead to only one cycle of fully reversed loading for fracture to occur), where for reinforcing steel this strain has a value in the range of  $\varepsilon_{pf} = 0.06$  to  $0.083$  as shown by the results plotted in Figure 1. The variability in the results can also be represented by a lognormal distribution with a lognormal standard deviation of 0.25.



(a)  $\varepsilon_{pf} = 0.06$  from test results given in  
Mander et al. (1994).

(b)  $\varepsilon_{pf} = 0.083$  from test results given in  
Brown and Kunnath (2004)

*Figure 1. Fatigue damage modelling based on tests from two different sources.*

The damage model in Eq. (2) can be generalized to incorporate multiple cycles of constant amplitude loading, or variable amplitude loading. If  $D_{cycle}$  is the damage incurred by one completely reversed cycle of loading for a specific cyclic amplitude, and if multiple random cycles exist, then Miner's hypothesis may be used to estimate the cumulative fatigue damage fraction ( $D_f$ ). The total damage may be found by normalizing all partial damage cycles to the maximum strain amplitude, and converting the total number of cycles into an effective number of constant amplitude cycles of loading ( $N_{eff}$ ) whereby there is damage equivalence between the constant amplitude cycles and variable amplitude cycles:

$$D_f = \sum D_i = \sum \left| \frac{\varepsilon_{ap}}{\varepsilon_{pf}} \right|_i^2 = N_{eff} \left| \frac{\varepsilon_{pm}}{\varepsilon_{pf}} \right|^2 \quad (3)$$

in which  $\sum D_i$  = summation of damage fractions for each of the  $i^{\text{th}}$  cycles;  $N_{eff}$  = the equivalent/effective number of constant amplitude cycles which is based on  $\varepsilon_{pm}$  = the peak plastic strain response for the loading history under consideration.

A reinforced concrete structure under dynamic excitation, will respond to the overall excitation from the foundation upwards—the foundation dynamically loads the structure as a whole, and the structural members resist the imposed loading. Large seismic loads induce *plastic displacements* in the structural members, which in turn produce *plastic rotations* within the plastic hinge zones that in turn result in *plastic curvatures* at the critical region of the plastic hinge, which finally cause *plastic strains* in the reinforcing bars at those critical hinge locations. The connection between plastic displacements, rotations, curvatures and strains can be related via geometric transformations, as given below. Therefore, Eq. (3) may be expanded accordingly as follows:

$$D_f = N_{eff} \left| \frac{\varepsilon_{pm}}{\varepsilon_{pf}} \right|^2 = N_{eff} \left| \frac{\phi_{pm}}{\phi_{pf}} \right|^2 = N_{eff} \left| \frac{\theta_{pm}}{\theta_{pf}} \right|^2 = N_{eff} \left| \frac{\Delta_{pm}}{\Delta_{pf}} \right|^2 \quad (4)$$

in which  $\phi_{pm}$ ,  $\theta_{pm}$ ,  $\Delta_{pm}$  are the maximum peak curvature, rotation and displacement response values for the load history under consideration, and  $\phi_{pf}$ ,  $\theta_{pf}$ ,  $\Delta_{pf}$  are the curvature, rotation and displacement parameters that are equivalent to a response that would lead to fatigue failure with only one completely reversed cycle of loading,  $N_f = 1.0$  in Eq. (2).

The parameters  $\varepsilon_{pf}$ ,  $\phi_{pf}$ ,  $\theta_{pf}$ ,  $\Delta_{pf}$  are interconnected via characteristic structural geometry attributes, the latter three of which are structure-specific. The evaluation of such parameters is considered in the following subsections in which relationships are developed starting from bar strain and subsequently transformed to global structure displacement.

For a structure that essentially behaves in a single degree of freedom fashion, such as the bridge presented in Figure 2, plastic strains and curvatures are connected by (Dutta and Mander, 2001):

$$\phi_p = 2\varepsilon_{ap}/D' \quad (5)$$

where  $D'$  = the pitch circle diameter of the longitudinal reinforcement in the bridge pier.

Plastic hinge rotations are connected to the plastic curvatures by:

$$\theta_p = \phi_p L_p \quad (6)$$

in which  $L_p$  = the equivalent plastic hinge length given by:

$$L_p = 0.08 L + 4400 \varepsilon_y d_b \quad (7)$$

where  $L$  = the column length;  $\varepsilon_y$  = yield strain of the longitudinal reinforcement; and  $d_b$  = diameter of the longitudinal bars.

The plastic displacement (drift) can be related to the plastic rotation of the column:

$$\Delta_p = \theta_p h_e \quad (8)$$

where  $h_e$  = height to the seismic centre of mass.

### Structural Fatigue Demand

Several methods are available for to convert each displacement response into equivalent constant amplitude fatigue cycles. Rain-flow methods are commonly used to decompose a random response into a

number of different amplitude-specific blocks of different mean stress for high cycle fatigue with non-zero mean stress. Chang and Mander (1994) developed energy-based cycle counting methods suited to inelastic spectra analysis and the energy-based fatigue rules given in Mander et al. (1994). Neither are applicable for the elastic spectra developed herein, instead two simple methods were investigated.

A normalization routine, referred to herein as RMC, where RM means “root mean” and  $C = -1/c$  in which  $c$  = the fatigue exponent that controls the relative importance placed on different amplitude response cycles, similar to a classic “peak picking” method, where each identified positive and negative peak is amplitude weighted to the power of  $C$ . The underlying principle is that the damage done by the variable amplitude loading is equivalent to an effective number of cycles  $N_{eff}$  for the maximum amplitude, in the present context this is the spectral displacement,  $S_d$ .

From Eq. (3), it follows that  $D_{const} = \sum D_i$ , where  $D_{const}$  = the damage by constant amplitude cycling; and  $\sum D_j$  = summation of damage fractions of the peaks for the variable amplitude history. Expanding in terms of individual peaks:

$$2N_{eff} \left| \frac{S_d}{S_u} \right|^C = \sum \left| \frac{X_j}{S_u} \right|^C \quad (9)$$

where  $2N_{eff}$  = the number of peaks/reversals in the history;  $S_u$  = the ultimate displacement peak for  $N_{eff}=1$ ; and  $X_j$  = the amplitude of the  $j^{\text{th}}$  peak of the random history. Thus the effective number of constant amplitude cycles is  $N_{eff}$ . To reduce the computational overhead of counting peaks, a more expedient approach is to consider every point,  $X_j$ , in the displacement history and correct for the fact that not all points are considered at the peak, giving this formulation for cycle counting:

$$N_{eff} = \frac{1}{2} \sum \left| \frac{X_j}{S_d} \right|^C = \frac{\Delta t}{T} \sum \left| \frac{B_c X_i}{S_d} \right|^C \quad (10)$$

in which  $\Delta t$  = the time-step length used in the elastic earthquake time-history analysis;  $T$  = the natural period of vibration for the case under consideration ( $T/\Delta t$  = the number of points in one cycle of motion); and  $B_c$  = the amplification factor, dependent on the exponent  $C$  such that one-cycle of constant amplitude motion gives a result of unity. For exponent values of  $C = 1, 2, 3$ , the amplification factors are  $B_{c=1} = \pi/2$ ,  $B_{c=2} = \sqrt{2}$ , and  $B_{c=3} = 4/3$ , respectively. For reinforcing-steel critical fatigue,  $C = 2$ . This approach is identical to the well-known root-mean-square (RMS) signal analysis technique. The cycle counting approach used herein is a development of, but remains similar to, that given in Dutta and Mander (2001).

## Bridge Structure Case Study

Figure 2 presents details of a bridge pier designed (Tanabe, 1999) conforming to New Zealand code requirements. The pier is 7 m high and is taken from a “long” multi-span highway bridge on firm soil with 40 m longitudinal span and 10 m transverse width. The weight of the super-structure reaction at each pier is assumed to be 7,000 kN. The bridge was designed for an earthquake with a spectral acceleration of 0.4g. This bridge has been the subject of previous studies on financial losses (Dhakal and Mander, 2006). It is re-examined herein for its proneness to seismic fatigue damage.

## Fatigue Damage Analysis: Interpretation of Results

Figures 3 presents the overall results for the low cycle fatigue investigation where the bridge described above is subjected to the 2010-2011 Canterbury Earthquake Sequence. The upper row of graphs in Figure 3 presents the acceleration-displacement response spectra (ADRS) in log-log space. In this way the diagonal lines plot the natural period of vibration for an elastic structure. Elastic response spectral results

are plotted for five different damping ratios: 5, 10, 15, 20 and 25 percent. The upper and lower curves are the results for 5 and 25 percent damping, respectively.

Also, plotted on each ADRS graph as a thick red line is the pushover capacity of the bridge pier such that the initial diagonal line falls on the natural period of the structure, while the horizontal plateau plots the plastic strength capacity. Over-plotted on the plastic capacity are blue bullets that show the response displacement amplitude for a prescribed level of equivalent viscous damping. The intersection of seismic demand and capacity gives the performance point denoted by the vertical dashed orange line with the spectral displacement (in mm) noted in red at the horizontal axis.

The second row of graphs in Figure 3 presents the results for the cyclic demand spectra computed using Eq. (10) with  $C = 2$ . The graph in the third of Figure 3 shows the total cyclic demand for all earthquakes in the 2010-2011 Canterbury Earthquake Sequence. Note the results are normed back to the maximum spectral displacement observed amongst all the earthquakes in the Sequence, as per Eq. (10), specifically the 22/2/2011 event; the largest earthquake in the Canterbury Earthquake Sequence.

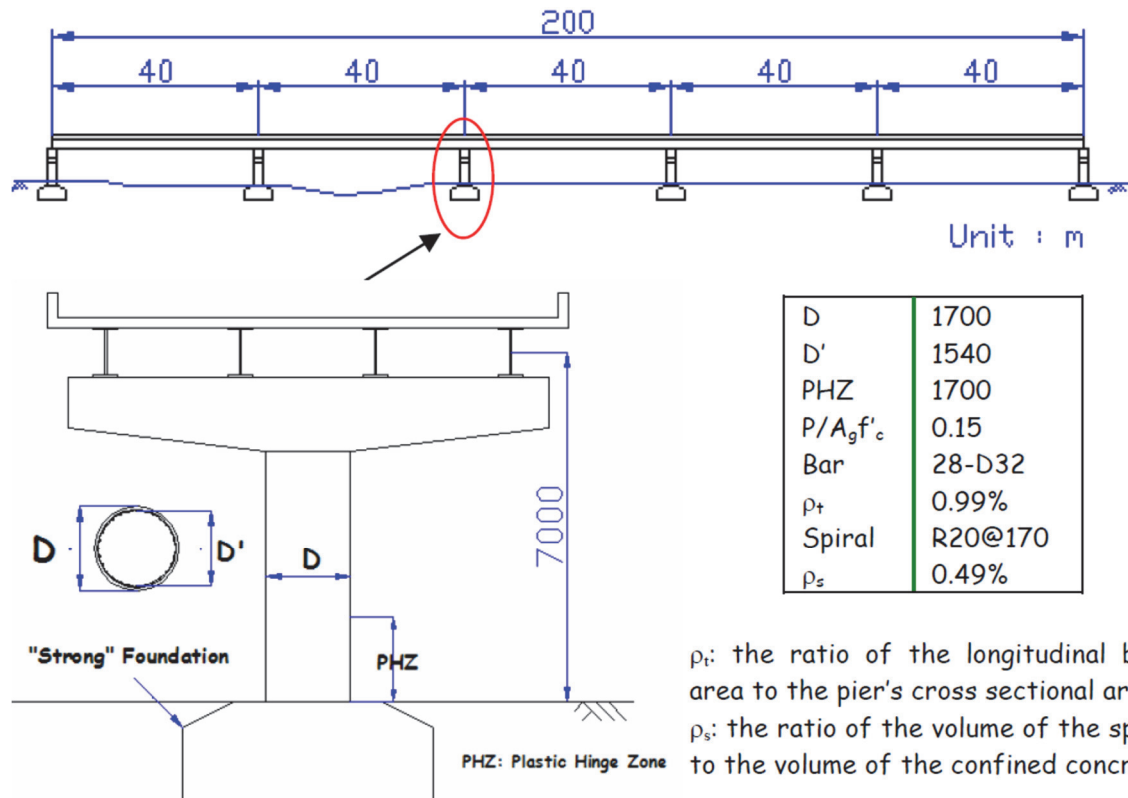


Figure 2. Bridge used in case study designed to New Zealand code provisions  
(Dhakal and Mander, 2006).

Superimposed on the fatigue demand spectra graphs (plotted in the second and third rows of Figure 3) is the cyclic fatigue capacity of the bridge structure represented by a thick diagonal red line. For a specified spectral amplitude, the red line provides the equivalent number of equi-amplitude cycles necessary to lead to first fatigue fracture of a longitudinal reinforcing bar in a pier column of the bridge. On that line is plotted an orange bullet and an associated number that indicates the *cyclic capacity* for that spectral displacement amplitude. Below that point at the same amplitude is a second orange coloured bullet point and number that represents the *cyclic demand* for the associated damping factor obtained from the ADRS

graph above. The ratio of the *cyclic demand* to the *cyclic capacity* gives the fatigue damage fraction ( $D_f$ ) with the results highlighted in yellow in the top right corner of each fatigue spectra graph.

### Fatigue Damage Analysis: Results for the Christchurch CBD

Figure 3 presents the results as if the bridge was located within the vicinity of the Christchurch CBD. For this location, results for two different earthquakes are given in Figure 3: (i) the initial Darfield earthquake on 4/9/2010 presented in the left column of graphs; and (ii) the largest of the Sequence, the Lyttelton Earthquake on 22/2/2011 presented in the right hand column of graphs.

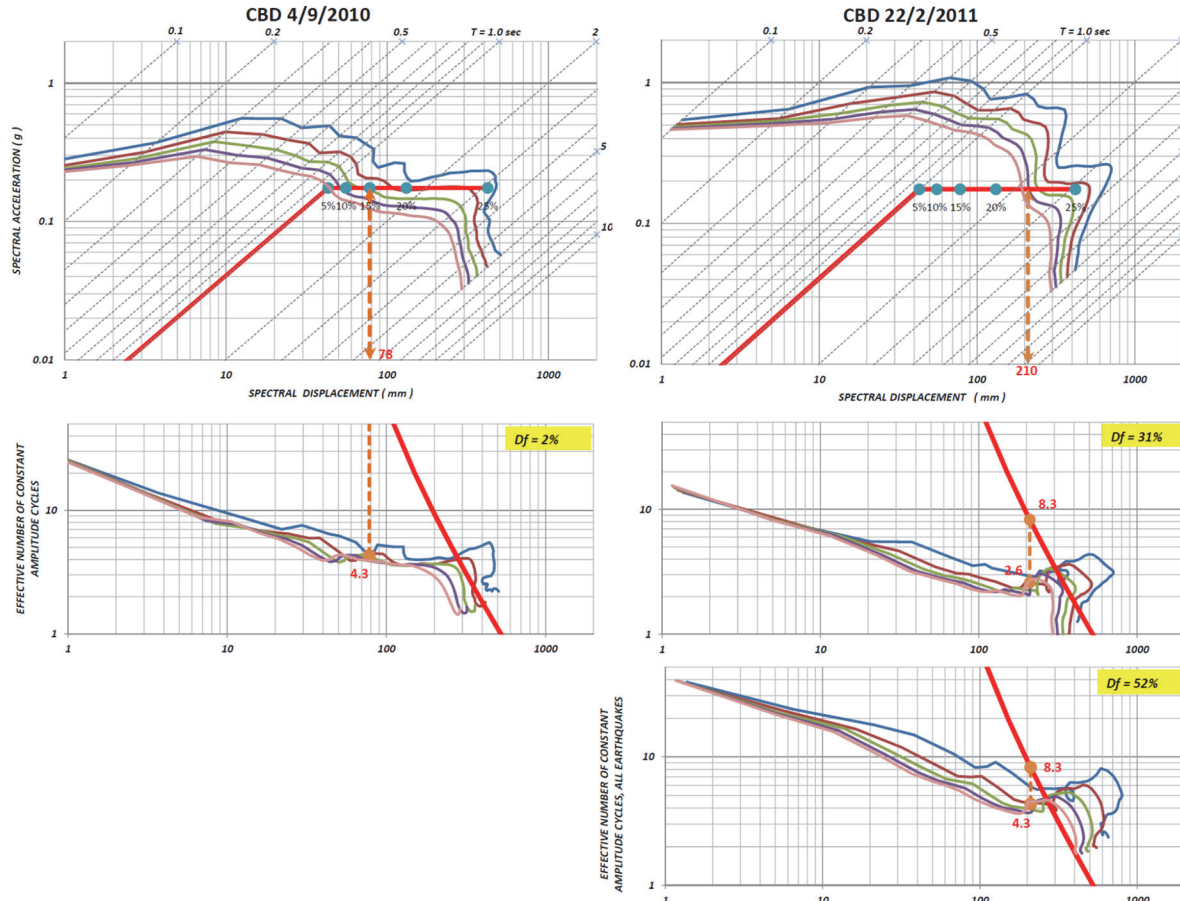


Figure 3. ADRS and Fatigue Spectra results for the bridge structure located within the vicinity of the Christchurch CBD subjected to the 2010-2011 Canterbury Earthquake Sequence

For structures within or nearby the Christchurch Central Business District (CBD) the four free-field GeoNet strong motion recording stations were considered. Specifically, these stations are the Christchurch Botanic Gardens (CBGS), Christchurch Cathedral College (CCCC), Christchurch Hospital (CHHC), Resthaven (REHS). Elastic response spectra were generated for each directional component for all CBD recordings.

For a structure in the general CBD region of Christchurch, instead of using all eight earthquake components individually, or any one component in isolation to draw conclusions, a composite approach whereby a single spectra is generated with known statistical (record-to-record variability) properties. Thus, representative statistics were generated from response results of the eight individual ground motion recordings for each of the four earthquake events. The response quantities of this type of spectral analysis

were assumed to conform to a log-normal distribution, characterized by two parameters: the median,  $\hat{x}$ ; and the dispersion factor  $\beta$  (the log-normal standard deviation).

The spectral displacement and number of effective fully reversed cycles of loading ( $S_d$ ,  $N_{eff}$ ) are computed for each specified natural period and damping factor ( $T$ ,  $\xi$ ). Thus the spectral values plotted in Figure 3 are a median (the 50<sup>th</sup> percentile) of the 8 available components of motion.

Results of analyses of several structures have shown that reinforcement fatigue was mostly restricted to the four largest ground motion events of the 2010-2011 Canterbury Earthquake Sequence. However, a majority of the fatigue demand came from the 22/2/2011 M6.3 Lyttelton Earthquake ground motion. In Figure 3, the fatigue modelling for the 4/9/2010 Darfield event gives the damage for that event alone, whereas for the 22/2/2011 Lyttelton event the two fatigue spectra are normed back to the spectral displacements of that event, as required in Eq. (10). The upper fatigue spectra gives the damage for that event alone, whereas the bottom right spectra gives the computed number of constant amplitude cycles aggregated over all events in the Canterbury Earthquake Sequence.

For the initial Darfield Earthquake of 4/9/2010 shown in the left column of Figure 3, a spectral displacement of 78 mm is inferred at the intersection of the seismic demand and the structural capacity from the ADRS. This is equivalent to a ductility factor of  $\mu=1.8$  and a damage fraction of  $D_f=2\%$  is inferred.

The largest earthquake in the CBD vicinity was the Lyttelton Earthquake of 22/2/2011 with the results shown in the right column of Figure 3. A displacement of 210 mm is inferred from the ADRS, implying a structure ductility factor of  $\mu=4.9$ . Using the associated fatigue spectra (right column, centre graph of Figure 3) a cyclic demand of 2.6 cycles is inferred for an associated fatigue capacity of 8.3 cycles. Thus for the main earthquake of 22/2/2011, a damage fraction of  $D_f=31\%$  was consumed. However, if cycles over all damaging earthquakes in the Canterbury Earthquake Sequence are included from 4/9/2010 to 23/12/2011 are considered then the number of cycles increases from  $N_{eff}=2.6$  to 4.3 to give a total sequence damage fraction of  $D_f=52\%$ .

## Discussion and Conclusion

New Zealand design codes have long recognised the cyclic loading demands imposed by earthquakes and have historically required structures to be capable of sustaining four completely reversed cycles of inelastic loading with a structure ductility factor of four. Consequently, buildings and bridges are designed for reduced strength to a structure-specific loadings code. Concrete structures are then prescriptively detailed in their potential plastic hinge zones for ductility; such detailing has been validated through analysis and testing to ensure ductility capability under cyclic loading effects.

Not so well understood at the time these codes were written, is the problem of low cycle fatigue and its adverse effect on the longitudinal reinforcement in particular, as well as the confinement steel (Dutta and Mander, 2001). If a single earthquake occurs and causes noticeable damage, then it is also likely that the cyclic effect of that event may have consumed some of the available fatigue resistance. Moreover, if several large earthquakes in a sequence have occurred, the question of low-cycle fatigue becomes more prominent. If the structure has sustained significant fatigue damage, restoration to an as-new condition may be difficult. As fatigue damage is irreparable, those damaged portions and their associated connections within the structure may be required to be rebuilt with new materials.

This paper has set forth a simple direct method of analysis to estimate the extent of low cycle fatigue damage to structures, and the longitudinal reinforcement in critical plastic hinge zones in particular, when subject to one or more earthquakes in a sequence.

To illustrate the fatigue analysis procedure and expected outcomes for the 2010-2011 Canterbury Earthquake Sequence, a case study of a simple bridge structure was presented for the Christchurch CBD. The inherent uncertainties in both the fatigue demand and resistance along with epistemic uncertainty associated with analysis simplifications were also considered.

Based on the analysis presented herein, it can be concluded that, for the considered bridge structure location within the Christchurch CBD, the initial Darfield event consumed only a minor amount (2%) of the fatigue life. If this were the only earthquake, such limited damage may be deemed *de minimis*, thereby not warranting restoration of that fatigue damage to as-new condition. However, the key Lyttelton earthquake of 2/22/2011 added another 30 percent of fatigue damage, and by the end of the sequence this increased to 52 percent; a condition that would require restoration of the particular fatigue damage.

## References

- Brown, J., and Kunnath, S.K., (2004) "Low-cycle fatigue failure of reinforcing steel bars." *ACI Materials Journal*, 101 (6): 457-466.
- Dhakal, R. P., and Mander, J. B., (2006) "Financial loss estimation methodology for natural hazards" *Bulletin of the NZ Society for Earthquake Engineering*, Vol. 39, No. 2, pp 91-105.
- Dutta, A., and Mander, J.B., (2001) "Energy Based Methodology for Ductile Design of Concrete Columns" *Journal of Structural Engineering*, ASCE, Vol 127 (12), pp 1374-1381.
- Kennedy, R. P., Cornell, C. A., Campbell, R. D., Kaplan, S., & Perla, H. F. (1980). "Probabilistic Seismic Safety Study of an Existing Nuclear Power Plant," *Nuclear Engineering and Design*, 59(2), 315-338. doi:10.1016/0029-5493(80)90203-4
- Mander, J.B, Panthaki, F. and Kasalanati, A. (1994). "Low-Cycle Fatigue Behavior of Reinforcing Steel." *Journal of Materials in Civil Engineering*, ASCE, 6(4): 453-468.
- Tanabe, T., (1999). "Comparative Performance of Seismic Design codes for Concrete Structures," Elsevier, New York, Vol. 1.